

# Accelerated Breast DCE-MRI using Compressed Sensing with Low Rank

Dong Wang

Nanjing University of Science and Technology

*311112253@njust.edu.cn*

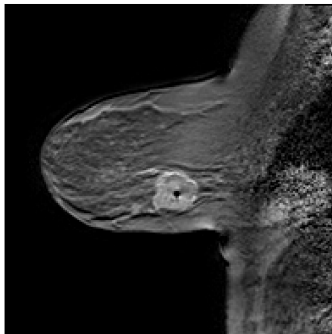
# Overview

- 1 Introduction
- 2 Background
- 3 Materials and Methods
- 4 Results and Discussions
- 5 Future Work

# Magnetic Resonance Imaging

- Magnetic Resonance (MR) imaging has been widely used in medical diagnosis, such as cancer and tumor, because of its non-invasive manner and accurate display of soft tissue changes.
- Dynamic MRI plays an important role in a number of clinical MR imaging applications, such as DCE(dynamic contrast-enhanced)-MRI and functional MRI.

# An Example of DCE-MRI



# DCE-MRI

- DCE-MRI provides critical information regarding tumor perfusion/permeability by the dynamic measurement of signal increase after injection of a  $T_1$  contrast agent (CA).
- DCE-MRI employs sequential acquisition of MR images after an intravenous injection of a CA.
- In the tissue region of interest, the CA usually arrives faster and in larger concentrations in well-perfused, highly vascular and permeable regions.
- DCE-MR image displays a characteristic time signal intensity change related to the CA concentration in the voxel.

# DCE modeling

- The vascular perfusion and permeability information of a tumor can be obtained from quantitative modeling of DCE data.
- Standard Toft-Kety Model is an effective model to estimate pharmacokinetic parameters such as  $K^{trans}$  and  $V_e$ .
- Both high temporal and spatial resolutions are required to obtain accurate and reproducible measurements of tumor perfusion/blood flow and permeability.
- However, the dynamic nature and signal-to-noise considerations of the DCE experiment limit simultaneous enhancement of temporal and spatial resolution by conventional data acquisition methods.

# Acceleration of imaging

- For the acceleration of dynamic MR images, a common strategy used to balance the trade-off between spatial and temporal resolution is to reduce k-space data at each frame.
- Various successive algorithms use this idea, such as keyhole, k-t Broad-use Linear Acquisition Speed-up Technique (k-t BLAST), SENSE etc.

# Compressed Sensing

- Compressed sensing theory shows that it is possible to accurately reconstruct the MR image from highly undersampled Fourier data, which results in significantly reduced scanning time.
- MRI obeys two key requirements for successful application of CS.
- Medical images are naturally sparse or compressible by sparse coding in an appropriate transform domain such as finite difference and wavelet transform.
- MRI scanners naturally acquire encoded samples, rather than direct pixel samples.



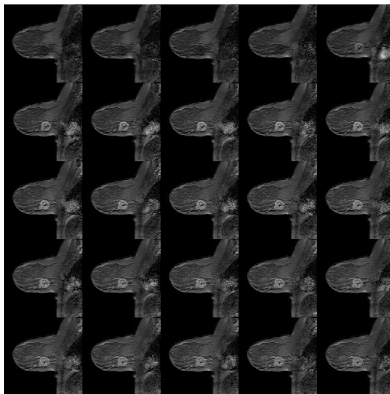
# Compressed Sensing

- Following CS theory, dynamic MR images can be reconstructed by solving an  $l_1$ -norm minimization problem in the sparse domain subject to data consistency constraint using fast algorithms such as IST (iterative shrinkage thresholding) and ADMM (Alternating direction method of multipliers).

# Low Rank

- The combination of compressed sensing and low-rank matrix completion represents an attractive proposition for further increases in imaging speed.
- For dynamic MRI, the background component corresponds to the highly correlated information among frames, which is slowly changing over time, resulting in the image matrix to be low rank.
- This means that dynamic MR images not only show sparsity in spatial domain, but also have redundancy in temporal domain.

# An Example of DCE-MRI



# Application

- Several applications of the CS theory to dynamic MRI have been successfully demonstrated such as k-t SPARSE, k-t FOCUSS, k-t GRAPPA etc.
- But only a few work on DCE-MRI data and almost none on breast.
- Thus DCE-MRI is still an appealing application of the CS algorithm.

1 Introduction

**2 Background**

3 Materials and Methods

4 Results and Discussions

5 Future Work

# Compressed Sensing

Compressed sensing has been used in MR image reconstruction successfully since it is born. The CS approach requires that:

- The desired images have a sparse representation in a known transform domain;
- The aliasing artifacts due to k-space undersampling be incoherent in the transform domain;
- A non-linear reconstruction be used to enforce both sparsity of the image representation and consistency with the acquired data.

# Models

For conventional CS-MRI, the formulation is as follows:

$$\hat{x} = \arg \min_x \frac{1}{2} \|Ax - b\|^2 + \alpha \|x\|_{TV} \quad (1)$$

where  $x$  is the 2D MR image we want to recover,  $A$  is the partial Fourier transform or sampling mask,  $b$  is the undersampled data in  $k$ -space, and  $\alpha$  is the weight of TV norm.

# TV norm

- Total Variation (TV) or finite difference based strategies, which were originally designed for denoising of images have recently gained wide interest for many MRI applications beyond denoising.
- TV norm is defined as  $\|x\|_{TV} = \sqrt{\Delta_1 x_{ij}^2 + \Delta_2 x_{ij}^2}$  where  $\Delta_1$  and  $\Delta_2$  are finite difference along the first and second coordinates respectively.
- TV models have the main benefit that they are very well suited to remove random noise, incoherent noise-like artifacts from random undersampling and streaking artifacts from undersampled sampling, while preserving the edges of the images.



# Wavelet

The improved version of Model (1) is obtained by having both a wavelet transform and a TV transform. The formulation is as follows:

$$\hat{x} = \arg \min_x \frac{1}{2} \|Ax - b\|^2 + \alpha \|x\|_{TV} + \beta \|Wx\|_1 \quad (2)$$

where  $W$  is 2-D wavelet transform matrix and  $\beta$  is the weight of wavelet transform.

# Algorithm

- Model (2) is based on the fact that MR image is piecewise smooth and is sparse in wavelet domain and should have small total variations.
- Model (2) can be solved by using FCSA (Fast composite splitting algorithm), which is an efficient algorithm for MR image reconstruction.

# Low Rank

- For dynamic MR images, redundancy not only appears in spatial domain but also appears in temporal domain.
- Low rank theory is very promising in making use of the redundancy and further accelerating imaging time.

# Model

In dynamic MRI, previous work on this combination proposed a solution that is both low-rank and sparse. The model k-t SLR is as follows:

$$\hat{x} = \arg \min_x \frac{1}{2} \|Ax - b\|^2 + \alpha \|x\|_{TV} + \beta \|x\|_* \quad (3)$$

where  $*$  is the nuclear norm of  $x$ , which is the sum of singular value of  $x$ .

# Model

In this model,  $x$  is rearranged as spatio-temporal matrix form to exploit correlations. For  $x \in R^{m \times n}$

$$x = \begin{bmatrix} x(p_0, t_0) & \dots & x(p_0, t_{n-1}) \\ \vdots & & \\ \vdots & & \\ x(p_{m-1}, t_0) & \dots & x(p_{m-1}, t_{n-1}) \end{bmatrix}$$

, where  $x(p_i, t_j)$  is the pixel in position  $i$  and frame  $j$ ,  $i = 0, \dots, m-1, j = 0, \dots, n-1$ . Under model (3), we show that the combination of low rank and TV also demonstrated great improvement on breast DCE-MRI data.

1 Introduction

2 Background

3 **Materials and Methods**

4 Results and Discussions

5 Future Work

# Data Collection

We apply this approach retrospectively to *in vivo* breast data acquired using a Philips (Best, Netherlands) Achieva 3T scanner with  $TR = 7.9$  ms,  $TE = 1.3$  ms, flip angle = 20 deg. The dimension of the original data is  $192 \times 192 \times 20 \times 1 \times 25$ , which consist of 20 slices and 25 dynamics.

# Preprocessing

- Two derived data sets were created: (A) a 5.5 fold randomly undersampled data set using the scheme below, and (B) a fully sampled data set with additional noise added at a level of 0.5% of the maximum intensity of the image.
- For both derived data sets, pharmacokinetic parameters ( $K^{trans}$  and  $V_e$ ) were estimated using the Standard Toft-Kety Model, and the concordance correlation coefficients (CCC) of the two parameters between the original data and the derived data were calculated.



# Undersampling

We generate a 2-D Cartesian sampling mask for dynamic MRI reconstruction. The dimension of the mask is  $192 \times 25$ . For each dynamic, low frequency region is fully sampled with the central window radius of 10 pixels. Outside the central window, we randomly pick a few lines along the phase encoding direction. The total acceleration of the mask is 5.5. Fig.1 shows one dynamic of the sampling mask.

# Mask

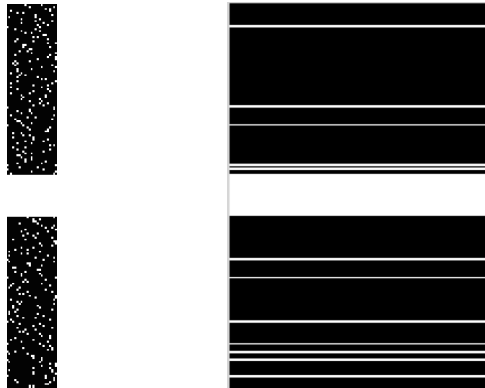


Fig 1. The 2-D sampling mask for all dynamic (left) and 2-D sampling for one dynamic (right). For every 2-D mask, the central is fully sampled and the periphery is randomly sampled. The total

# Reconstruction

We solve model (3) using the alternating direction method of multipliers, which is an efficient algorithm for convex optimization problems with more than one constraint.

$$\begin{aligned} \hat{x} = \arg \min_{x, S, L} \quad & \frac{1}{2} \|Ax - b\|^2 + \alpha \|S\|_1 + \beta \|L\|_*, \\ \text{s.t. } & S = TV(x); x = L. \end{aligned} \quad (1)$$

# Reconstruction

We solve the equation using its unconstrained version using  
Argumented Lagrange method, where we minimize

$$F_{\alpha,\beta}(x, S, L) = \frac{1}{2} \|Ax - b\|^2 + \alpha \|S\|_1 + \beta \|L\|_* + \\ \frac{\lambda_1}{2} \|S - TV(x)\|^2 + \frac{\lambda_2}{2} \|L - x\|^2$$

# Reconstruction

We solve the equation above using a three-step alternating minimization scheme below, where in each step we only solve one variable assuming the rest to be known

$$x_{n+1} = \arg \min_x \frac{1}{2} \|Ax - b\|^2 + \frac{\lambda_1}{2} \|S_n - TV(x)\|^2 + \frac{\lambda_2}{2} \|L_n - x\|^2$$

$$S_{n+1} = \arg \min_S \|S - TV(x_{n+1})\|^2 + \frac{2\alpha}{\lambda_1} \|S\|_1$$

$$L_{n+1} = \arg \min_L \|L - x_{n+1}\|^2 + \frac{2\beta}{\lambda_2} \|L\|_*$$

# Reconstruction

- Similar alternating direction methods are widely used in compressed sensing and low rank minimization problems. We solve each subproblem in different ways.
- The first subproblem is quadratic and we solve it using conjugate gradient method with back-tracking line search.
- The second subproblem requires joint processing of finite difference operator in three different dimensions, thus we use multidimensional shrinkage algorithm.
- For the third subproblem, it is similar to the form of standard nuclear norm minimization problem. We solve it using IST (Iterative singular value thresholding), which is a very efficient algorithm for solving nuclear minimization problem and can be generalized to non-convex spectral constraints.

# Reconstruction

The singular value shrinkage is defined as

$$\mathbb{S}_{\beta/\lambda_2}(x_{n+1}) = \sum_{i=0}^{\min(m,n)} (\sigma_i - \lambda_2 \sigma_i / \beta)_+ u_i v_i^*$$

Here,  $u_i$ ,  $v_i$ , and  $\sigma_i$  are the singular vectors and values of  $x_{n+1}$ , respectively. The thresholding function is defined as

$$(\sigma)_+ = \begin{cases} \sigma, & \text{if } \sigma \geq 0 \\ 0, & \text{else} \end{cases} \quad (2)$$

# Overview

- 1 Introduction
- 2 Background
- 3 Materials and Methods
- 4 Results and Discussions**
- 5 Future Work



## Results

Fig 2 and Fig 3 shows the result of reconstructions of one dynamic and all dynamics respectively with the acceleration of 5.5. Some blurring has occurred, but the CS image is far better than the zero-filled reconstruction. Fig 4 and Fig 5 show the CCC plots for  $K_{trans}$  and  $V_e$  between the original and the CS reconstruction and between the original and the data with added noise. The CCC for  $K_{trans}$  and  $V_e$  were 0.85 and 0.93 respectively, for both case. Notably, the general pattern of scatter appears remarkably similar.

# Results

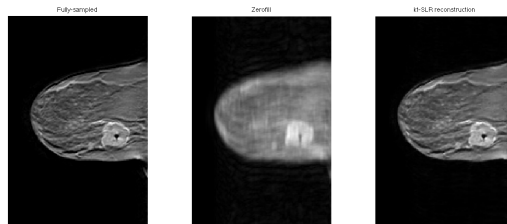


Fig.2 Result of reconstruction of one dynamic. The image on the left is the fully sampled data. The image in the middle is zerofill image. The image on the right is the reconstruction using the proposed algorithm with the acceleration of 5.5

# Results

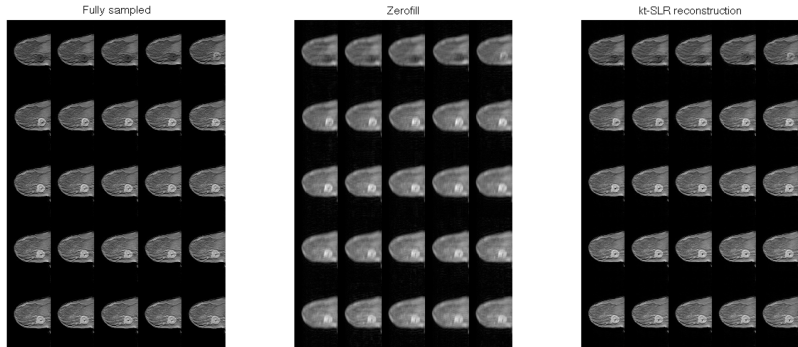


Fig.3 Result of reconstruction of all dynamics. The image on the left is the fully sampled data. The image in the middle is zerofill image. The image on the right is the reconstruction using the proposed algorithm with the acceleration of 5.5.

# Results

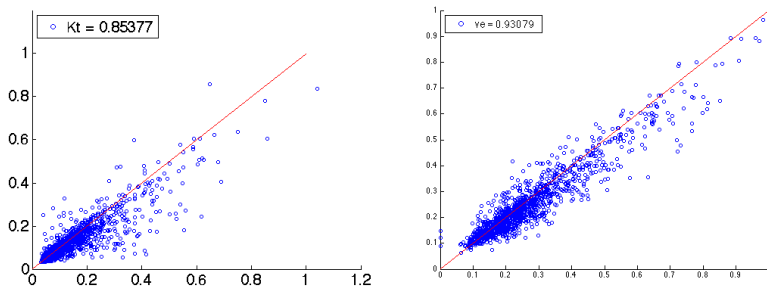


Fig 4 (DataA) The concordance correlation between (left) and  $v_e$  (right) generated from fully sampled data and from using kt-SLR. The CCCs of  $K_t$  and  $v_e$  were 0.85 and 0.93 respectively.

# Results

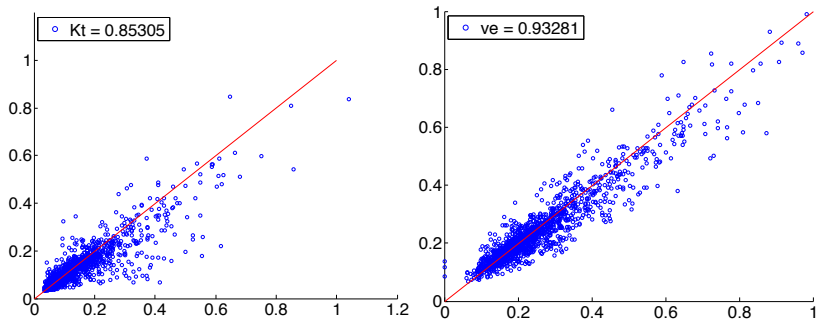


Fig 5 (DataB) The concordance correlation between (left) and  $ve$  (right) generated from fully sampled data and after adding 0.5% noise corruption. The CCCs of  $Kt$  and  $ve$  were 0.85 and 0.93 respectively.

# Discussion

A typical 2D DCE-MRI acquisition might use a SENSE factor of 2 and a partial Fourier factor of 0.6, for an effective 3.3 undersampling. Here we achieve a 5.5 undersampling with a loss in parameter accuracy roughly equivalent to 0.5% noise corruption. While a loss in parameter accuracy in isolation is bad, the additional information that  $5.5/3.3 = 67\%$  more dynamics could provide may outweigh this effect. In fact, if the additional dynamics were simply time averaged, then the SNR would increase by 29%, which would more than compensate for the equivalent 0.5% signal loss due to the CS undersampling.

## 1 Introduction

## 2 Background

## 3 Materials and Methods

## 4 Results and Discussions

## 5 Future Work

# Future Work

## Combination with dictionary learning

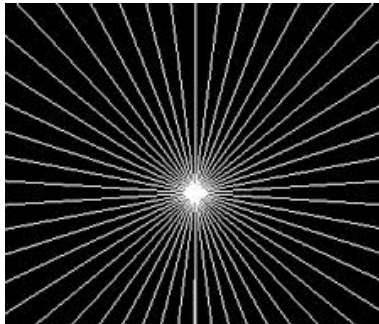
- Dictionary learning is a very promising method to sparsify medical images.
- Combination of dictionary learning and compressed sensing in medical images is still challenging problem.
- Many useful algorithms to train dictionary for medical images, such as K-SVD, MOD etc.



## Future Work

Non-Cartesian undersampling patterns, such as spiral and radial lines.

- Apart from Cartesian masks, non-Cartesian masks are getting more and more attentions these years.
- radial undersampling lines

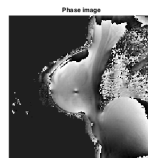
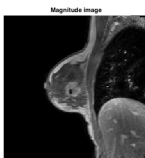
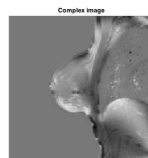
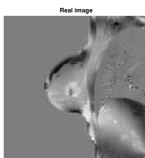


## Future Work




Consideration of phase information of MR images.

- The above applications of CS framework assume that both magnitude and phase of the voxels are sparse, however, this is not always the case for fast acquisitions because the phase of the voxel is not null when the echo time is away from the RF pulse and there are inhomogeneities in the main field.
- In many MRI applications, including DCE-MRI and fMRI, one expects most of the signal information of interest to be contained in the magnitude value, whereas the phase values are expected to vary smoothly spatially.
- Indeed, some methods have even constrained the phase to be zero, but this is often unrealistic in practice since there can be residual phase components that are non-negligible but spatially smooth.

# Phase Image



# Reference

-  David Donoho, Compressed sensing. (IEEE Trans. on Information Theory, 52(4), pp. 1289 - 1306, April 2006)
-  Emmanuel Cands, Justin Romberg, and Terence Tao, Robust uncertainty principles: Exact signal reconstruction from highly incomplete frequency information. (IEEE Trans. on Information Theory, 52(2) pp. 489 - 509, February 2006)
-  Michael Lustig, David Donoho, and John M. Pauly, Sparse MRI: The application of compressed sensing for rapid MR imaging. (Magnetic Resonance in Medicine, 58(6) pp. 1182 - 1195, December 2007)

## Compressed Sensing MRI

- ◀ ◻ ▶ ◀ ◻ ▶ ◀ ≡ ▶ ◀ ≡ ▶ ≡

# The End